DMD Fast Forward. Published on September 22, 2017 as DOI: 10.1124/dmd.117.077313
This article has not been copyedited and formatted. The final version may differ from this version.

RNA-Seq Profiling of Intestinal Expression of Xenobiotic Processing Genes in Germ-Free Mice

Zidong Donna Fu, Felcy P Selwyn, Julia Yue Cui, Curtis D. Klaassen

Affiliations:

Department of Environmental and Occupational Health Sciences, University of Washington, Seattle (Z.D.F, F.P.S, J.Y.C, C.D.K)

Running title: Intestinal Expression of XPGs in germ-free mice

Corresponding author:
Curtis D. Klaassen, PhD
Department of Environmental and Occupational Health Sciences
School of Public Health
University of Washington
4225 Roosevelt Way NE, Suite #100
Seattle, WA 98105. Box 354695
Email: curtisklaassenphd@gmail.com

Text pages: 43
Tables: 4
Figures: 10
References: 41
Number of words in Abstract: 250
Number of words in Introduction: 576
Number of words in Discussion:1514

Abbreviations:

Abc: ATP-binding cassette; Adh: alcohol dehydrogenase; AhR: aryl hydrocarbon receptor; Akr: aldo-keto reductase; Aldh: aldehyde dehydrogenase; Aox: aldehyde oxidase; As_3mt: arsenic (+3 oxidation state) methyltransferase; Asbt: apical sodium-dependent bile acid transporter; Bal: bile acid-CoA ligase; Bat: bile acid-CoA:amino acid *N*-acyltransferase; Bcrp: breast cancer resistance protein; Bsep: bile salt export pump; CAR: constitutive androstane receptor; Cbr: carbonyl reductase; Ces: carboxylesterases; Cnt: concentrative nucleoside transporter; Comt: catechol *O*-methyltransferase; CV: conventional; duo: duodenum; Ephx: epoxide hydrolase; Ent: equilibrative nucleoside transporter; Fmo: flavin monooxygenase; FPKM: fragments per kilobase of exon per million reads mapped; FXR: farnesoid X receptor; Gclc: glutamate-cysteine ligase catalytic subunit; Gclm: glutamate-cysteine ligase modifier subunit; GF: germ-free; Glyat: glycine-*N*-acyltransferase; Gst: glutathione-*S*-transferase; HNF: hepatocyte nuclear factor; ile: ileum; jej: jejunum; LI: large intestine; liv: liver; Mat: methionine adenosyltransferase; Mate: multidrug and toxin extrusion protein; Mdr: multidrug resistance protein; Mrp: multidrug resistance-associated protein; Nat: *N*-acetyl transferase; Nqo: NAD(P)H: quinone oxidoreductase; NR: nuclear receptor; Nrf2: nuclear factor erythroid 2-related factor 2; Ntcp: Na+-taurocholate cotransporting polypeptide; Oat: organic anion transporter; Oatp: organic anion-transporting polypeptide; Oct: organic cation transporter; Octn, organic cation/carnitine transporter; Ost: organic solute transporter; P450: cytochrome P450; Papss: 3'-phosphoadenosine 5'-phosphosulfate synthase; Pept: peptide transporter; Pon: paraoxonase; Por: P450 (cytochrome) oxidoreductase; PPAR: peroxisome proliferator-activated receptor; PXR: pregnane X receptor; RNA-Seq: RNA-Sequencing; RT-qPCR: reverse transcription-quantitative real-time polymerase chain reaction; RXR: retinoid X receptor; SAMe: *S*-adenosylmethionine; Slc: solute carrier; Slco: solute carrier organic anion; Sult: sulfotransferase; TF: transcription factor; Tpmt: thiopurine *S*-methyltransferase; UDPGA: Uridine diphosphate glucuronic acid; Ugdh: UDP-glucose 6-dehydrogenase; Ugp2: UDP-glucose pyrophosphorylase 2; Ugt: UDP-glucuronosyltransferase; XPG: xenobiotic-processing gene.

ABSTRACT

Intestinal bacteria can affect xenobiotic metabolism through both direct bacterial enzyme-catalyzed modification of the xenobiotics and indirect alterations of the expression of host genes. To determine how intestinal bacteria affect the expression of host xenobiotic-processing genes (XPGs), the mRNA profiles of 303 XPGs were characterized by RNA-sequencing in four intestinal sections and compared to that in the liver from adult male conventional (CV) and germ-free (GF) mice. 54 XPGs were not expressed in the intestine of either CV or GF mice. GF condition altered the expression of 116 XPGs in at least one intestinal section, but had no effect on 133 XPGs. Many cytochrome P450s such as Cyp1a, 2b10, 2c, and most 3a members, as well as carboxylesterase 2a were expressed lower in the intestine of GF than CV mice. In contrast, GF mice had higher intestinal expression of some phase-I oxidases (alcohol dehydrogenase 1, aldehyde dehydrogenase 1l1 and 4a1, as well as flavin monooxygenase 5) and phase-II conjugation enzymes (UDP-glucuronosyltransferase 1a1 and sulfotransferase 1c2, 1d1, and 2b1). Several transporters in the intestine exhibited higher expression in GF mice, such as bile acid transporters (apical sodium-dependent bile acid transporter, organic solute transporter α and β), peptide transporter 1, and multidrug and toxin extrusion protein 1. In conclusion, lack of intestinal bacteria alters the expression of a large number of XPGs in the host intestine, some of which are section-specific. Cyp3a is down-regulated in both liver and intestine of GF mice, which probably contributes to altered xenobiotic metabolism by intestinal bacteria.

Introduction

Trillions of microbes inhabit the human intestine, collectively known as the intestinal microbiota, and form a complex ecological community that influences normal physiology and disease susceptibility (Lozupone et al., 2012). The intestinal bacteria are beneficial for host metabolism, aid in digestion, produce vitamins B and K, and contribute to normal immune function, thereby creating a symbiotic relationship with the host (Tremaroli and Backhed, 2012). It has been increasingly recognized that intestinal bacteria are implicated in several diseases, such as obesity, diabetes, neurologic diseases, inflammatory bowel disease, cancer, and liver diseases (Fu and Cui, 2017).

Metabolism of orally administered drugs by intestinal bacteria can alter the efficacy and toxicity of drugs (Klaassen and Cui, 2015). A wide range of metabolic reactions are performed by intestinal bacteria, such as hydrolysis, reduction, dehydroxylation, decarboxylation, dealkylation, dehalogenation, deamination, heterocyclic ring fission, aromatization, nitrosamine formation, acetylation, esterification, isomerization, and oxidation (Mikov, 1994). Intestinal bacteria-mediated metabolism of biliary-excreted metabolites is often crucial to the enterohepatic circulation of xenobiotics. Bacterial enzymes in the intestine often make drugs more lipophilic by deconjugating conjugated drug metabolites, favoring intestinal uptake and increasing the half-life of drugs (Stojancevic et al., 2014). According to the PharmacoMicrobiomics database, approximately 60 drugs are known to be affected by intestinal microbes (Rizkallah et al., 2012). Some well-known examples include the analgesic acetaminophen (by *Clostridium difficile*), cardiotonic drug digoxin (by *Eggerthella lenta*), antiviral drug sorivudine (by *Bacteroides*), hypnotic nitrazepam (by *Clostridium leptum*),

and anthelminitic levamisole (by *Bacteroides* and *Clostridium spp.*) (Klaassen and Cui, 2015; Jourova et al., 2016). The wide yet less controlled use of intestinal bacteria modulators (prebiotics, probiotics, synbiotics, and antibiotics) can be problematic in polypharmacy, due to bacteria-mediated alteration of the pharmacokinetics and pharmacodynamics of concomitant orally administered drugs. Humans have marked variation in microbiota inhabiting their intestine as evidenced by metagenomic studies (Human Microbiome Project, 2012), and may help to explain inter-individual variations in the pharmacokinetics of xenobiotics. Thus, understanding the functions of individual microbial populations and how the intestinal microbiota varies across age, gender, ethnicity, life styles, health or disease states, and medications of humans, is emerging as a novel component of personalized medicine.

In addition to the direct bacterial enzyme-catalyzed metabolism, intestinal bacteria can also affect the biotransformation of xenobiotics via an indirect mechanism of regulating the expression of host XPGs. Modulation of intestinal bacteria has been shown to alter the hepatic and renal expression of genes involved in drug metabolism and disposition, evidenced by GF, probiotic-, or antibiotic-treated animals (Bjorkholm et al., 2009; Toda et al., 2009; Selwyn et al., 2015b; Kuno et al., 2016; Selwyn et al., 2016). Given the crucial role of intestinal tissue in xenobiotic absorption and metabolism, as well as its close proximity to the microbiota in the lumen, it is of great importance to determine the effect of intestinal bacteria on the expression of xenobiotic metabolism-related genes in the intestine.

In this study, GF mice that do not have microbes, as well as CV counterparts, were employed to investigate the role of intestinal bacteria on host gene expression.

RNA-sequencing was applied to provide comprehensive and unbiased mRNA profiles of various XPGs, including phase-I and phase-II drug metabolizing enzymes, drug uptake and efflux transporters, as well as related transcription factors. These results will advance our knowledge on the regulation of host drug metabolism by intestinal bacteria and shed light on the underlying mechanisms for food-drug and drug-drug interactions, as well as inter-individual differences in xenobiotic metabolism.

Materials and Methods

Animals. All mice used in the studies were male C57BL/6 mice at 2-3 months of age (n = 3) due to the known effect of age and gender on XPG expression (Cui et al., 2012a; Fu et al., 2012). All mice were housed in an AAALAC (Association for Assessment and Accreditation of Laboratory Animal Care International)-accredited facility at the University of Kansas Medical Center (KUMC), with a 14-h light/10-h dark-cycle, in a temperature and humidity-controlled environment. All mice were given *ad libitum* access to autoclaved rodent chow #5K67 (LabDiet, St. Louis, MO) and autoclaved water. The initial breeding colony of GF C57BL/6J mice was established with mice purchased from the National Gnotobiotic Rodent Resource Center (University of North Carolina at Chapel Hill). GF mice were born and raised inside sterile isolators and received sterile feed, water, and bedding. All CV mice were purchased from the Jackson Laboratory (Bar Harbor, ME). All animal experiments were approved by the Institutional Animal Care and Use Committee at KUMC.

Tissue collection. Animals were not fasted due to the known effect of nutritional status on XPG expression (Fu and Klaassen, 2014). All tissues were harvested between 9:00 am and noon. Intestinal contents were flushed with ice-cold phosphate buffered saline, and intestinal tissues were separated into various sections, namely duodenum (duo), jejunum (jej), ileum (ile), and large intestine (LI). Liver and intestinal sections were snap-frozen in liquid nitrogen and stored at -80˚C before further analysis.

Total RNA Isolation. Total RNA was isolated from tissues using RNA-Bee reagent (Tel-Test Inc., Friendswood, TX) following the manufacturer's protocol. The concentration of total RNA in each sample was quantified spectrophotometrically at

260nm using a NanoDrop 1000 Spectrophotometer (Thermo Scientific, Waltham, MA). RNA integrity was confirmed using a dual Agilent 2100 Bioanalyzer (Agilent Technologies Inc., Santa Clara, CA), and the samples with RNA integrity numbers above 7.0 were used for the following experiments.

cDNA library preparation and RNA-Seq. The cDNA library preparation and sequencing of the transcriptome were performed in the KUMC Genome Sequencing Facility. The cDNA libraries from total RNA samples (n = 3/group) were prepared using an Illumina TruSeq RNA sample prep kit (Illumina, San Diego, CA). Three micrograms of total RNA were used as the RNA input according to recommendations of the manufacturer's protocol. The mRNAs were selected from the total RNAs by purifying the poly-A containing molecules using poly-T primers. The RNA fragmentation, first and second strand cDNA syntheses, end repair, adaptor ligation, and PCR amplification were performed according to the manufacturer's protocol. The average size of the cDNAs was approximately 160 bp (excluding the adapters). The cDNA libraries were validated for RNA-integrity and quantity using an Agilent 2100 Bioanalyzer (Agilent Technologies Inc., Santa Clara, CA) before sequencing. The cDNA libraries were clustered onto a TruSeq paired-end flow cell and sequenced (2×50 bp) using a TruSeq SBS kit (Illumina, San Diego, CA) on an Illumina HiSeq2000 sequencer with a multi-plexing strategy of 4 samples per lane.

RNA-Seq Data Analysis. After the sequencing platform generated the sequencing images, the pixel-level raw data collection, image analysis, and base calling were performed by Illumina's Real Time Analysis (RTA) software on a Dell PC attached to a HiSeq2000 sequencer. The base call files (*.BCL) were converted to qseq files by

the Illumina's BCL Converter, and the qseq files were subsequently converted to Fastq files for downstream analysis. The RNA-Seq reads from the Fastq files were mapped to the mouse reference genome (UCSC mm10), and the splice junctions were identified by TopHat2. The output files in BAM (binary sequence alignment) format were analyzed by Cufflinks to estimate the transcript abundance. Differential expression analysis between CV and GF mice was determined using Cuffdiff (significant at a false discovery rate with Benjamini-Hochberg adjustment FDR-BH<0.05). The mRNA abundance was expressed as fragments per kilobase of exon per million reads mapped (FPKM). RNA-seq data are uploaded to NCBI's Gene Expression Omnibus database with accession number GSE102867.

Statistical Analysis. Data are presented as mean FPKM ± standard error of mean (S.E.M.). XPGs with mean FPKM values per tissue less than 1 in each of the four sections of the intestine were defined as not expressed in intestine. Differences between CV and GF mice that were significant by Cuffdiff (FDR-BH<0.05) were represented with asterisks. Hepatic expression of the XPGs in CV and GF mice was reported previously (Selwyn et al., 2015b) and included in this manuscript to compare the effect of GF condition on the liver to that in the various sections of the intestine. To compare the expression of XPGs in intestine of CV and GF mice, a two-way hierarchical clustering dendrogram (Ward's minimum variance method, distance scale) was generated by JMP 12.1.0 software (SAS Institute, Inc., Cary, NC) on the mean mRNA expression of XPGs with differential expression in at least one section of the intestine between CV and GF mice (FDR-BH<0.05, Cuffdiff). The expression of each individual gene was standardized among eight experimental groups, to present the differential

expression pattern of multiple genes between CV and GF mice in various sections of the intestine. Relatively high mRNA abundance is represented in red, whereas relatively low mRNA abundance is in blue. Relative color intensities are not comparable among genes.

Results

mRNA Expression of all XPGs in Intestine of CV and GF Mice.

In total, 303 XPGs with known important functions in xenobiotic metabolism and transport were analyzed. These genes belong to various categories as reported previously (Fu et al., 2016), namely 158 phase-I enzymes, 78 phase-II enzymes, 35 uptake transporters, 21 efflux transporters, and 11 transcription factors (TFs). Among these 303 XPGs, 116 XPGs had differential expression (DE) between CV and GF mice in at least one section of the intestine (FDR-BH<0.05, Cuffdiff). This includes 69 phase-I enzymes, 27 phase-II enzymes, 17 transporters, and 3 transcription factors (Table 1). Table 2 lists 54 XPGs that are not expressed (NE) in the intestine of CV or GF mice (FPKM<1 in all sections of the intestine). Table 3 lists 133 XPGs with no differential expression (NDE) between CV and GF mice in the intestine (FDR-BH≥0.05, Cuffdiff).

In order to determine the tissue-specific expression patterns of the 116 differentially expressed XPGs, a two-way hierarchical clustering dendrogram was generated using their standardized mean FPKM values (Fig. 1). These XPGs partitioned into four distinctive expression patterns, namely large intestine- (cluster 1), ileum- (cluster 2), duodenum- (cluster 3), as well as duodenum and jejunum-enriched (cluster 4). In general, XPGs within the same intestinal section clustered together regardless of phenotype, indicating that sections of the intestine was a more predominant regulatory factor in XPG expression than phenotype. Among all 4 sections of the intestine, duodenum was the section where most of the XPGs were highest expressed in both CV and GF mice. The effect of lack of intestinal bacteria on XPG expression was specific to intestinal sections. Certain XPGs within the same family also

exhibited similar expression alteration patterns by lack of intestinal bacteria. For example, multiple Cyp2d subfamily members (Cyp2d9, 2d10, 2d12, 2d13, and 2d34) had higher expression in large intestine of GF mice (cluster 1); multiple Cyp3a subfamily members (Cyp3a11, 3a25, 3a44, and 3a59) had lower expression in duodenum of GF mice (cluster 3); and multiple Akr1cs (Akr1c12, 1c13, and 1c19) were expressed higher in duodenum and large intestine of GF mice (cluster 4). The FPKMs of individual XPGs of each gene family are further described below.

Intestinal Expression of Phase-I Enzymes in GF Mice.

Phase-I enzymes Involved in Hydrolysis Reactions. There are three major families of xenobiotic hydrolytic enzymes, including **c**arboxylesterases (Cess) for esters and amides; paraoxonases (Pons) for organophosphates, aromatic carboxylic acid esters, cyclic carbonates, and lactones; as well as epoxide hydrolases (Ephxs) for electrophilic epoxides. In total, 18 Cess, 3 Pons, and 4 Ephxs were investigated in this study. Ces1a, 2f, 4a, 5a, and Ephx3 were not expressed in intestine of CV or GF mice (Table 2). Ces1b, 1c, 2e, 2h, 3a, 3b and all three Pons (Pon1-3) did not show differential intestinal expression between CV and GF mice (Table 3). Eight Cess and 3 Ephxs had differential expression between CV and GF mice in at least one section of the intestine (Table 1). As shown in Figure 2, four hydrolases showed higher intestinal expression in GF mice, such as Ces1e in jej (51%) and LI (67%), Ces1f in jej (40%), as well as Ces1g (168%) and Ces2c (29%) in LI. In contrast, six hydrolases were lower in GF mice, such as Ces1d in duo (36%), Ephx1 in duo (58%) and jej (42%), Ces2a in all four sections of the intestine (duo 76%; jej 56%; ile 61%; LI 74%), Ces2b in jej (39%), Ces2g in ile (45%) and LI (40%), and Ephx4 in LI (50%). Ephx2 had higher expression

in jej (64%) and LI (118%) but lower expression in ile (46%) of GF mice. Similar to the liver data, Ces1g had higher expression in LI of GF mice. Probably of greatest significance is that Ces2a had lower expression in intestine as well as liver of GF mice. In contrast to the similar expression of some Cess and Ephxs in liver of CV and GF mice, some genes had higher (Ces1e, 1f, 2c) or lower (Ces1d, 2b, 2g, Ephx1, 4) expression in intestine of GF mice. Some genes (Ces3b and 4a) with differential expression in liver remained unchanged in intestine of GF mice.

Phase-I enzymes Involved in Reduction Reactions. Three major families of xenobiotic reductases were investigated, namely 16 aldo-keto reductases (Akrs) from 6 subfamilies that metabolize aldehydes and ketones, 4 carbonyl reductases (Cbrs) that metabolize carbonyl-containing xenobiotics, and 2 NAD(P)H:quinone oxidoreductases (Nqos) that metabolize quinones. Akr1c21 and both Nqos (Nqo1 and Nqo2) were not expressed in intestine of CV or GF mice (Table 2). The intestinal expression of 8 Akrs (1a4, 1b3, 1b10, 1c6, 1c20, 1d1, 1e1, and 7a5) and 2 Cbrs (Cbr2 and Cbr4) showed no differences in expression between CV and GF mice (Table 3). Seven Akrs and 2 Cbrs had differential expression between CV and GF mice in at least one section of the intestine (Table 1). Seven out of nine reductases showed higher intestinal expression in GF mice, such as Akr1b7 in jej (136%); Akr1c12 (84%; 60%; 41%), Akr1c13 (152%; 104%; 48%), Akr1c14 (29%; 71%; 58%) in jej, ile, and LI; Akr1c18 in LI (741%); Akr1c19 in all four sections of the intestine (101%; 241%; 211%; 158%); and Cbr1 in jej (41%), whereas a couple of reductases were expressed lower in GF mice, namely Akr1b8 (49%) and Cbr3 (32%) in LI (Figure 3). In contrast to the similar expression of some Akrs in liver of CV and GF mice, some genes had higher (Akr1b7, 1c12, 1c13,

1c14, 1c18, Cbr1) or lower (Akr1b8, Cbr3) expression in intestine of GF mice. Substrates of Akr1c12, 1c13, and 1c19 were likely to be affected the most by the lack of intestinal bacteria, because the expression of these genes was higher in the intestine, and there was an increase in expression of these genes in multiple intestinal sections.

Phase-I enzymes Involved in Oxidation Reactions.

Cytochrome P450s (P450s). P450s, a class of heme-containing monooxygenases, are major enzymes for the biotransformation of numerous endobiotics as well as the detoxification or bioactivation of various xenobiotics (e.g. drugs, chemical carcinogens, and environmental chemicals) (Danielson, 2002; Parkinson et al., 2013). P450 (cytochrome) oxidoreductase (Por) is an important electron donor for P450s to facilitate their catalytic functions. The intestinal expression of 76 P450s in the Cyp1-4 families as well as Por were investigated. There were 11 P450s that were not expressed in the intestine of CV or GF mice (Table 2). As detailed in Table 3, 35 P450s did not show any differences in intestinal expression between CV and GF mice. Thirty P450s and Por had differential expression between CV and GF mice in at least one section of the intestine (Table 1). Eleven out of thirty P450s had lower intestinal expression in GF mice, including Cyp1a1 in all three sections of small intestine (87%; 92%; 97%), Cyp1b1 in jej (45%), Cyp2b10 in duo (57%) and ile (74%), Cyp2c29 in ile (90%), Cyp2c55 in all four sections of intestine (76%; 66%; 79%; 55%), Cyp2e1 in jej (58%), Cyp2j9 in ile (39%), Cyp3a11 in duo (60%) and ile (86%), Cyp3a25 in duo (51%) and ile (78%), Cyp3a44 in duo (58%), and Cyp3a59 in duo (49%) and ile (77%) (Figure 4). Some genes showed higher expression in GF mice, such as Cyp2c38 (141%), Cyp2c44 (97%), Cyp2c67 (43%), and Cyp2c68 (43%) in jej, Cyp2d9 (142%)

and Cyp2d34 (39%) in LI, Cyp2d10 in duo (69%) and LI (114%), Cyp2d12 (65%) and Cyp2d13 (87%) in LI, Cyp2d26 (65%; 163%) and Cyp3a13 (67%; 124%) in jej and LI, Cyp4b1 in all four sections of intestine (91%; 216%; 62%; 127%), Cyp4v3 in jej (88%) and LI (100%), as well as Por in jej (38%). In addition, Cyp2c65 and 2c66 had section-specific differential expression between CV and GF mice, which is an increase in one section and decrease in another section. In contrast to the similar expression of some P450s in liver of CV and GF mice, some genes had higher (Cyp2c44, 2d9, 2d10, 2d12, 2d26, 2d34, 3a13, 4b1, 4f13, 4v3) or lower (Cyp1a1, 1b1, 2c29, 2j9, 3a25) expression in intestine of GF mice. Some genes with differential expression in liver (Cyp1a2, 2a5, 2a22, 2b29, 2c39, 2c40, 2c50, 2c54, 2c69, 3a16, 4a12b, 4a14, 4a31, 4a32, 4f17) remained unchanged in intestine of GF mice. Some genes (Cyp2b10, 2c38, 2c55, 2c67, 2c68, 2d13, 3a11, 3a44, 3a59, and Por) had similar alterations of expression in liver and intestine of GF mice. Probably the most important change is the decrease in Cyp3a subfamily, because the decrease was observed in intestine and liver, and Cyp3a subfamily metabolizes over 50% of drugs. Substrates of Cyp1a1, 2b10, and 2c55 were likely to be metabolized more slowly with the lack of intestinal bacteria, because they were primarily expressed in the intestine, where they were expressed at lower levels in GF mice. Most of the Cyp4 enzymes were expressed at a higher level in liver than intestine (Cyp4a10, 4a12b, 4a14, 4a31, 4a32), whereas Cyp4b1 was expressed higher in intestine and was also increased in GF mice.

Non-P450 oxidation. Four families of non-P450 enzymes that mediate xenobiotic oxidation were investigated, including 6 alcohol dehydrogenases (Adhs) for ethanol and other aliphatic alcohols, 20 aldehyde dehydrogenases (Aldhs) for

aldehydes, 3 aldehyde oxidases (Aoxs) for aromatic aldehydes, and 5 flavin monooxygenases (Fmos) for xenobiotics with nucleophilic atoms. Aox3l1 and Fmo3 were not expressed in intestine of CV or GF mice (Table 2). As detailed in Table 3, 11 Aldhs did not show any differences in intestinal expression between CV and GF mice, in addition to Aox1, 3, and Fmo1. Six Adhs, 9 Aldhs, and 3 Fmos had differential expression between CV and GF mice in at least one section of the intestine (Table 1). As shown in Figure 5, 12 out of 18 oxidases had higher intestinal expression in GF mice, such as Adh5 in LI (45%), Adh7 in jej (148%), Aldh1a1 in jej (52%) and LI (291%), Aldh1a7 (88%) and Aldh1b1 (43%) in LI, Aldh1l1 (103%), Aldh3a2 (34%), and Aldh3b1 (89%) in jej, and Aldh4a1 in duo (195%) and jej (458%), Fmo2 in duo (75%), Fmo4 in jej (28%), and Fmo5 in jej (70%) and LI (205%). Some genes had lower expression in GF mice, such as Adhfe1 in jej (58%) and Aldh18a1 in duo (44%). In addition, Adh1, 4, and 6a were higher in jej (192%; 64%; 114%), but lower in ile (53%; 73%; 52%); Aldh1l2 was higher in duo (261%), but lower in LI (60%). In contrast to the similar expression in liver of CV and GF mice, some genes had higher (Adh5, 7, Aldh1a1, 1a7, 1l1, 3a2, 3b1, 4a1, Fmo4) or lower (Adhfe1, Aldh18a1) expression in intestine of GF mice. Aox1 had differential expression in liver but remained unchanged in intestine of GF mice. Some genes (Aldh3a2, Fmo2, 5) had similar alterations of expression in liver and intestine of GF mice. Aldh1b1 had lower expression in liver but higher expression in LI of GF mice. Because none of the Adhs, Aldhs, or Fmos had consistently higher or lower expression in all sections of the GF mice, it is not likely these changes will have marked changes on the metabolism of their substrates.

The Intestinal Expression of Phase-II Enzymes in GF Mice.

Xenobiotics can be conjugated by phase-II enzymes with glucuronic acid (by UDP-glucuronosyltransferases or Ugts), sulfate (by sulfotransferases or Sults), glutathione (by glutathione-*S*-transferases or Gsts), or amino acids (by amino acid-conjugation enzymes), as well as methyl (by methyltransferases) or acetyl group (*N*-actyltransferases or Nats). In this study, 18 Ugts, 17 Sults, 25 Gsts, 3 methyltransfersases (catechol *O*-methyltransferase or Comt, arsenic methyltransferase or As_3mt, thiopurine *S*-methyltransferase or Tpmt), 3 Nats, and 3 amino acid-conjugation enzymes (bile acid-CoA ligase/Bal, bile acid-CoA:amino acid *N*-acyltransferase/Bat, and glycine-*N*-acyltransferase/Glyat) were investigated. Four Ugts, 10 Sults, 2 Gsts, as well as Nat1 and 3 were not expressed in the intestine of CV or GF mice (Table 2). As detailed in Table 3, some genes did not show any differences in intestinal expression between CV and GF mice, including 9 Ugts, 2 Sults, 11 Gsts, 3 methyltransferases (Comt, As_3mt, and Tpmt), as well as 3 amino acid-conjugation enzymes (Bal, Bat, and Glyat). Five Ugts, 5 Sults, 12 Gsts, and Nat2 had differential expression between CV and GF mice in at least one section of the intestine (Table 1). As shown in Figure 6 and 7, 13 out of 23 phase-II enzymes had higher expression in distinct intestinal sections of GF mice, such as Ugt1a1 (415%), Ugt2b5 (197%), and Ugt2b36 (106%) in LI, Ugt2a3 in jej (85%), Ugt2b38 in duo (129%), Sult1b1 (74%) and Sult1d1 (49%) in jej, Sult2b1 in jej (105%) and ile (47%), Gsta4 in jej (49%), Gstm7 in jej (82%), Gsto1 in jej (41%) and LI (44%), Gstp1 in jej (46%), and Nat2 in jej (45%). Some genes had lower expression in GF mice, such as Sult4a1 in jej (50%), Gsta3 in LI (35%), Gstm1, m3, and m4 in duo (66%; 64%; 58%) and ile (49%; 68%; 45%). In addition, Sult1c2, Gsta1, k1, m6, and t1 had section-specific differential expression

between CV and GF mice. In contrast to similar expression in liver of CV and GF mice, some genes had higher (Ugt1a1, 2a3, 2b5, 2b36, Sult2b1, Nat2, Gsta4, m7, o1) or lower (Sult4a1, Gsta3, m1, m3, m4) expression in intestine of GF mice. Some genes (Ugt2b35, 2b37, Sult1a1, 5a1, Gstp2, t2, t3) had differential expression in liver of the CV and GF mice, but remained unchanged in intestine of GF mice. Some genes (Sult1b1, 1d1) had similar alterations of expression in liver and intestine of GF mice. Ugt2b38 had lower expression in liver but higher expression in duo of GF mice. Some Ugts (Ugt1a1, 2a3) had comparable expression in intestine and liver, whereas most Ugts (Ugt2b5, 2b35, 2b36, 2b37, 2b38) had much lower expression in intestine than liver. Substrates of some Sults (Sult1b1, 1d1, 2b1) and Gsts (Gsta1, m3, o1) are likely to be affected by the lack of intestinal bacteria, because they were expressed at higher levels in intestine than liver, and the expression of these genes were altered in the intestine of GF mice.

Several enzymes involved in the synthesis of phase-II conjugation co-substrates were also investigated, including UDP-glucose pyrophosphorylase 2/Ugp2 (for UDP-glucose synthesis), UDP-glucose 6-dehydrogenase/Ugdh (for the synthesis of the glucuronidation cosubstrate UDPGA), 3'-phosphoadenosine 5'-phosphosulfate synthases/Papss (for the synthesis of the sulfation cosubstrate 3'-phosphoadenosine 5'-phosphosulfate/PAPS), glutamate-cysteine ligase catalytic/Gclc) and modifier/Gclm subunits (for the synthesis of Gst cosubstrate glutathione), and methionine adenosyltransferases/Mats (for the synthesis of the common methyl donor *S*-adenosylmethionine/SAMe). The intestinal expression of five of these enzymes, namely Ugp2, Papss1, Mat1a, 2a, and 2b, was not different between CV and GF mice (Table

3). Compared to CV mice, GF mice had higher intestinal expression of other genes, including Ugdh in jej (59%) and LI (93%), Papss2 in jej (182%), Gclc in ile (47%) and LI (36%), and Gclm in jej (44%) (Figure 8). In contrast to similar expression in liver of CV and GF mice, Papss2 and Gclm had higher expression in intestine of GF mice. Some genes (Ugp2, Mat1a) had differential expression in liver but remained unchanged in intestine of GF mice. Ugdh and Gclc had opposite patterns of altered expression in liver and intestine of GF mice. Because none of these genes had constant higher or lower expression in all sections of the GF mice, it is not likely these changes will have marked changes on the synthesis of these co-substrates for phase-II conjugation.

The Intestinal Expression of Xenobiotic Transporters in GF Mice.

Transporters with importance in xenobiotic transport were investigated, including 36 uptake transporters and 20 efflux transporters. Thirteen uptake transporters and 2 efflux transporters were not expressed in intestine of CV or GF mice (Table 2). Twelve uptake transporters and twelve efflux transporters did not have differential expression between CV and GF mice in the intestine (Table 3). As shown in Figure 9, 8 out of 17 transporters had higher expression in intestine of GF mice, such as peptide transporter 1 (Pept1/Slc15a1) in jej (179%) and LI (65%); organic cation/carnitine transporters Octn1/Slc22a4 in LI (507%) and Octn2/Slc22a5 in jej (16%), organic anion transporting polypeptide 2a1 (Oatp2a1/Slco2a1) in jej (22%) and LI (46%); multidrug resistance-associated protein 2 (Mrp2/Abcc2) in jej (51%); multidrug and toxin extrusion transporter 1 (Mate1/Slc47a1) in duo (72%) and jej (162%); and organic solute transporters (Ostα/Slc51a and Ostβ/Slc51b) in LI (18-fold; 208%). Some transporters had lower intestinal expression in GF mice, such as organic cation transporter 1 (Oct1/Slc22a1;

25%) in duo, organic cation transporter 3 (Oct3/Slc22a3; 47%), equilibrative nucleoside transporter 4 (Ent4/Slc29a4; 54%), organic anion transporting polypeptide 3a1 (Oatp3a1/Slco3a1; 41%), and multidrug resistance-associated protein 7 (Mrp7/Abcc10; 22%) in jej. In contrast to similar expression in liver of CV and GF mice, some transporters had higher (Pept1, Octn2, Mate1, Ostα, Ostβ) or lower (Oct1, Ent4, Otap3a1, Mrp7) expression in intestine of GF mice. Some transporters (Ntcp, Ent1, Oatp1b2, Abcg5, Abcg8) had altered expression in liver of GF mice but remained unchanged in intestine of GF mice. Some genes (Octn1, Mrp2) had similar alterations of expression in liver and intestine of GF mice. Some genes (Oct3, Oatp2a1) had opposite patterns of altered expression in liver and intestine of GF mice. Because none of the transporters had constant higher or lower expression in all sections of the GF mice, it is not likely these changes will have marked changes on the transport of their substrates.

The Intestinal Expression of Xenobiotic-Related Transcription Factors in GF Mice.

Various transcription factors (TFs) that are involved in the transcriptional regulation of XPGs were also investigated in this study, including the aryl hydrocarbon receptor (AhR), constitutive androstane receptor (CAR/Nr1i3), farnesoid X receptor (FXR/Nr1h4), hepatocyte nuclear factors (HNF1α and HNF4α/Nr2a1), peroxisome proliferator-activated receptor alpha (PPARα/Nr1c1), pregnane X receptor (PXR/Nr1i2), three retinoid X receptors (RXRα/Nr2b1, RXRβ/Nr2b2, and RXRγ/Nr2b3), and nuclear factor erythroid 2-related factor 2 (Nrf2). As shown in Figure 10, some TFs showed higher expression in GF mice, such as PPARα (31%) and PXR (15%) in jej. CAR

appeared to be expressed higher in GF than CV mice in all three sections of the small intestine (although not statistically significant), but lower expression in LI of GF mice. In contrast to similar expression in liver of CV and GF mice, FXR was expressed lower in jej (57%) but higher in LI (79%) of GF mice. Some TFs appeared to have lower expression in LI of GF mice, but did not achieve statistical significance. HNF1α and HNF4α did not have differential expression in intestine of CV and GF mice. In contrast to higher expression in liver of GF mice, AhR and Nrf2 expression in intestine remained similar between CV and GF mice.

Discussion

The present study was the first to investigate how lack of intestinal bacteria regulates the expression of host genes involved in drug metabolism and transport in the intestine. Comparing GF with CV mice, this study has demonstrated that the lack of intestinal bacteria alters the gene expression of a number of phase-I and phase-II drug metabolizing enzymes as well as transporters in the intestine (Table 1), and the altered pattern of XPG expression in intestine induced by the lack of intestinal bacteria differs from that in the liver.

To provide a condensed picture focusing on the genes altered the most, XPGs with over 5-fold differential expression in GF vs CV mice in at least one intestinal section are listed in Table 4, which includes 8 phase-I enzymes, 1 phase-II enzyme, and 3 transporters. Six of these are P450s that are responsible for the biotransformation of approximately 75% of drugs (Guengerich, 2008). Noticeably, CYP3A, which is present in critical drug-metabolic tissues such as liver and intestine, metabolizes more drugs than any other P450 (Wilkinson, 1996). In this study, the majority of Cyp3a subfamily members have lower intestinal expression in GF mice compared with CV mice, including Cyp3a11, 3a16, 3a25, 3a44, and 3a59 (Figure 4). Similarly, these Cyp3a members have markedly lower expression in livers of GF mice (Figure 4), which is consistent with previous reports (Toda et al., 2009; Kuno et al., 2016). In contrast, Cyp3a13 is the only Cyp3a member whose expression is higher in intestine of GF mice (Figure 4). It is known that the Cyp3a13 gene locates in a distinct position away from the Cyp3a locus on chromosome 5, where all other Cyp3a members cluster (Zaphiropoulos, 2003; Cui et al., 2012b). It is likely that Cyp3a13 and the other Cyp3a

members may have a different regulatory mechanism for expression due to this distinct gene location. Moreover, many other P450s show lower expression in GF mice compared to CV mice, such as the Cyp1a, Cyp2b10, and Cyp2c subfamily (Cyp2c29, 2c55, and 2c66), whereas a couple of P450s (Cyp2d26, 4b1, and 4v3) have higher expression in GF mice (Figure 4). The current finding of altered P450 expression in intestine of GF mice suggests that intestinal bacteria play an important role in regulating P450-mediated first-pass metabolism by the host intestine.

In addition to P450s, several other phase-I drug metabolizing enzymes are regulated by intestinal bacteria. Intestine-enriched Ces2a are carboxylesterases for large alcohol or small acyl groups, such as the cancer prodrug irinotecan (Humerickhouse et al., 2000; Zhang et al., 2012). This study shows that Ces2a has markedly lower expression in intestine of GF mice compared with CV mice (Figure 2), indicating a possible role of intestinal bacteria in the hydrolysis and activation of prodrugs mediated by host carboxylesterases of the intestine. The AKR1C subfamily members are ketosteroid reductases that play crucial roles in the metabolism of steroid hormones and prostaglandins, as well as metabolic activation of the polycyclic aromatic hydrocarbon carcinogens, and inactivation of nicotine derived nitrosaminoketones (Penning and Drury, 2007). This study reveals that several Akr1c subfamily members (Ark1c12, 1c13, 1c14, 1c18, and 1c19) have higher expression in intestine of GF than CV mice (Figure 3), indicating that the lack of intestinal bacteria may trigger the upregulation of the metabolism of steroid hormones and xenobiotics by the intestine. ALDH4A1 is a host enzyme involved in proline conversion to glutamate (Marchitti et al., 2008). Proline has been shown to be an important carbon and nitrogen source for the

growth of Gram-negative bacteria, which can convert proline to glutamate entering the tricarboxylic acid cycle (Krishnan and Becker, 2006). This study identifies increased intestinal expression of Aldh4a1 in GF mice (Figure 5), which suggests that proline metabolism pathway of the host intestine is induced as a result of lack of intestinal bacteria.

The expression of some phase-II enzymes in intestine is also affected by the intestinal bacteria. UGT1A1 catalyzes the glucuronidation of bilirubin and the chemotherapeutic drug irinotecan, and UGT1A1 polymorphism is implicated in Gilbert's syndrome, Crigler-Najjar syndrome, and irinotecan toxicity (Sugatani, 2013). Glucuronidates can be de-conjugated by beta-glucuronidases in the intestinal bacteria and then enter the enterohepatic circulation. Of note, Ugt1a1 expression in large intestine is markedly higher in GF mice compared with CV mice (Figure 6). It is possible that when the intestinal bacteria are absent, the large intestine increases its glucuronidation to reduce the recycling of chemicals in the enterohepatic circulation.

Intestinal bacteria are responsible for producing secondary bile acids from primary bile acids through deconjugation, dehydroxylation, epimerization, and oxidation (Fu et al., 2014; Wahlstrom et al., 2016; Li et al., 2017). It is known that GF mice have diminished secondary bile acids, but more total and conjugated bile acids in the intestine (Sayin et al., 2013; Selwyn et al., 2015a). The current study shows that bile acid transporters have higher expression in the intestine of GF mice compared with CV mice, specifically Asbt in ileum and large intestine and Ostα/Ostβ in the large intestine (Figure 9). This finding suggests an upregulation of bile acid intestinal reabsorption when intestinal bacteria are absent.

The expression of TFs in the intestine appears to be differentially regulated by intestinal bacteria. PXR and CAR are two master regulators of drug metabolism and their target drug metabolizing genes in intestine have been reported (Hartley et al., 2004; Park et al., 2016). The current study shows that intestinal bacteria-mediated changes in expression profiles of PXR and CAR in intestine are not consistent with the changes of their prototypical target genes Cyp3a11 and Cyp2b10, respectively (Figures 4 and 10). Other xenobiotic-sensing TFs, AhR and Nrf2, have similar expression in intestine between CV and GF mice, inconsistent with decreased expression of AhR target gene Cyp1a1 and increased expression of some Gsts that are targets of Nrf2. Therefore, the XPG alterations by lack of intestinal bacteria may not mediated by a single TF.

Previous publications indicate that microbial metabolites (such as short-chain fatty acids and tryptophan-metabolites), sensing through xenobiotic receptors PXR and AhR, can regulate host intestinal barrier function and innate immunity (Jin et al., 2014; Venkatesh et al., 2014; Ranhotra et al., 2016; Lanis et al., 2017). The present study has compared the intestinal expression profiles between CV and GF mice of target genes of PXR (Cui and Klaassen, 2016) and those of AhR (Sartor et al., 2009) as previously reported. The marked lower expression of PXR target genes Cyp3a11, Cyp2b10, as well as Gstm1, 3, 4 in the intestine of GF mice than CV mice (Figures 4 and 7) theoretically could be due to less activation of PXR. However, an exception to this includes some PXR target genes (such as Oatp1a4 and Mrp3) with similar intestinal expression between CV and GF mice (Table 3). Similarly, AhR target gene Cyp1a1 expression in the intestine of GF mice is lower than CV mice, whereas other target

genes Cyp1a2 and Aldh3a1 have similar intestinal expression between CV and GF mice (Figure 4 and Table 3). Therefore, it does not appear that alterations in PXR or AhR signaling pathway are responsible for the upregulation and downregulation of XPGs in GF mice. The exact mechanism for XPG alterations by intestinal bacteria remains elusive.

Lack of intestinal bacteria leads to similar alterations of some XPGs in liver and intestine, but different alterations of other XPGs in intestine from that in liver. Compared to CV mice, GF mice have lower expression of Cyp3a11 and Cyp2b10 in liver (Selwyn et al., 2015b) and similarly lower expression in duodenum and ileum (Figure 4), but their expression in jejunum and large intestine are similar in CV and GF mice (Figure 4). Several phase-II enzymes that are not differentially expressed in liver of GF and CV mice, have higher intestinal expression in GF mice, such as Ugt1a1, 2a3, Sult1c2, 2b1, and Gsto1 (Figures 6 and 7). In contrast, some enzymes with higher (Sult1a1, Gstt2, Gstt3) or lower (Gstp1, Gstp2) hepatic expression in GF mice, are not differentially expressed in intestine of CV and GF mice (Figures 6 and 7).

One should be cautious that mRNA level does not necessarily correlate with protein function. The protein levels and enzyme/transporter activities of XPGs were not determined in this study due to technique limitations. Specific antibodies and substrates of many isoforms of drug metabolizing enzymes and transporters are not available. Technical breakthroughs in proteomics and metabolomics are essential to determine the protein levels and activities of these enzymes and transporters. Furthermore, further studies are needed in the future to specify which genera of intestinal microflora

and which bacterial metabolites are responsible for the regulation of host gene expression.

In conclusion, the present study has demonstrated that despite many exceptions, lack of intestinal bacteria decreases expression of numerous P450s (Table 4), but increases phase-2 enzymes and transporters in intestine, which both help decrease the formation of reactive metabolites and elimination of chemicals. This reveals the important role of intestinal bacteria on host drug metabolism in an indirect manner and provides insights into the interaction between intestinal bacteria and pharmaceuticals. Furthermore, this finding paves a new path for exploring individual differences in pharmacokinetics from a metagenomic perspective.

Acknowledgements

The authors thank Clark Bloomer of the KUMC genomic sequencing facilities for his technical assistance on RNA-Seq.

Authorship Contributions

Participated in research design: Cui, Klaassen.

Conducted experiments: Selwyn, Cui.

Performed data analysis: Fu, Cui, Klaassen.

Wrote or contributed to the writing of the manuscript: Fu, Cui, Klaassen.

References

Bjorkholm B, Bok CM, Lundin A, Rafter J, Hibberd ML, and Pettersson S (2009) Intestinal microbiota regulate xenobiotic metabolism in the liver. *PLoS One* **4:**e6958.

Cui JY, Aleksunes LM, Tanaka Y, Fu ZD, Guo Y, Guo GL, Lu H, Zhong XB, and Klaassen CD (2012a) Bile acids via FXR initiate the expression of major transporters involved in the enterohepatic circulation of bile acids in newborn mice. *Am J Physiol Gastrointest Liver Physiol* **302:**G979-996.

Cui JY and Klaassen CD (2016) RNA-Seq reveals common and unique PXR- and CAR-target gene signatures in the mouse liver transcriptome. *Biochim Biophys Acta* **1859:**1198-1217.

Cui JY, Renaud HJ, and Klaassen CD (2012b) Ontogeny of novel cytochrome P450 gene isoforms during postnatal liver maturation in mice. *Drug Metab Dispos* **40:**1226-1237.

Danielson PB (2002) The cytochrome P450 superfamily: biochemistry, evolution and drug metabolism in humans. *Curr Drug Metab* **3:**561-597.

Fu ZD, Csanaky IL, and Klaassen CD (2012) Effects of aging on mRNA profiles for drug-metabolizing enzymes and transporters in livers of male and female mice. *Drug Metab Dispos* **40:**1216-1225.

Fu ZD and Cui JY (2017) Remote sensing between liver and intestine: importance of microbial metabolites. *Current Pharmacology Reports* **3:**101-113.

Fu ZD, Cui JY, and Klaassen CD (2014) Atorvastatin induces bile acid-synthetic enzyme Cyp7a1 by suppressing FXR signaling in both liver and intestine in mice. *J Lipid Res* **55:**2576-2586.

Fu ZD and Klaassen CD (2014) Short-term calorie restriction feminizes the mRNA profiles of drug metabolizing enzymes and transporters in livers of mice. *Toxicol Appl Pharmacol* **274:**137-146.

Fu ZD, Selwyn FP, Cui JY, and Klaassen CD (2016) RNA sequencing quantification of xenobiotic-processing genes in various sections of the intestine in comparison to the liver of male mice. *Drug Metab Dispos* **44:**842-856.

Guengerich FP (2008) Cytochrome p450 and chemical toxicology. *Chem Res Toxicol* **21:**70-83.

Hartley DP, Dai X, He YD, Carlini EJ, Wang B, Huskey SE, Ulrich RG, Rushmore TH, Evers R, and Evans DC (2004) Activators of the rat pregnane X receptor differentially modulate hepatic and intestinal gene expression. *Mol Pharmacol* **65:**1159-1171.

Human Microbiome Project C (2012) Structure, function and diversity of the healthy human microbiome. *Nature* **486:**207-214.

Humerickhouse R, Lohrbach K, Li L, Bosron WF, and Dolan ME (2000) Characterization of CPT-11 hydrolysis by human liver carboxylesterase isoforms hCE-1 and hCE-2. *Cancer Res* **60:**1189-1192.

Jin UH, Lee SO, Sridharan G, Lee K, Davidson LA, Jayaraman A, Chapkin RS, Alaniz R, and Safe S (2014) Microbiome-derived tryptophan metabolites and their aryl

hydrocarbon receptor-dependent agonist and antagonist activities. *Mol Pharmacol* **85:**777-788.

Jourova L, Anzenbacher P, and Anzenbacherova E (2016) Human gut microbiota plays a role in the metabolism of drugs. *Biomed Pap Med Fac Univ Palacky Olomouc Czech Repub* **160:**317-326.

Klaassen CD and Cui JY (2015) Review: mechanisms of how the intestinal microbiota alters the effects of drugs and bile acids. *Drug Metab Dispos* **43:**1505-1521.

Krishnan N and Becker DF (2006) Oxygen reactivity of PutA from Helicobacter species and proline-linked oxidative stress. *J Bacteriol* **188:**1227-1235.

Kuno T, Hirayama-Kurogi M, Ito S, and Ohtsuki S (2016) Effect of intestinal flora on protein expression of drug-metabolizing enzymes and transporters in the liver and kidney of germ-free and antibiotics-treated mice. *Mol Pharm* **13:**2691-2701.

Lanis JM, Alexeev EE, Curtis VF, Kitzenberg DA, Kao DJ, Battista KD, Gerich ME, Glover LE, Kominsky DJ, and Colgan SP (2017) Tryptophan metabolite activation of the aryl hydrocarbon receptor regulates IL-10 receptor expression on intestinal epithelia. *Mucosal Immunol*.

Li WK, Li H, Lu YF, Li YY, Fu ZD, and Liu J (2017) Atorvastatin alters the expression of genes related to bile acid metabolism and circadian clock in livers of mice. *PeerJ* **5:**e3348.

Lozupone CA, Stombaugh JI, Gordon JI, Jansson JK, and Knight R (2012) Diversity, stability and resilience of the human gut microbiota. *Nature* **489:**220-230.

Marchitti SA, Brocker C, Stagos D, and Vasiliou V (2008) Non-P450 aldehyde oxidizing enzymes: the aldehyde dehydrogenase superfamily. *Expert Opin Drug Metab Toxicol* **4:**697-720.

Mikov M (1994) The metabolism of drugs by the gut flora. *Eur J Drug Metab Pharmacokinet* **19:**201-207.

Park S, Cheng SL, and Cui JY (2016) Characterizing drug-metabolizing enzymes and transporters that are bona fide CAR-target genes in mouse intestine. *Acta Pharm Sin B* **6:**475-491.

Parkinson A, Ogilvie BW, Buckley DB, F. K, Czerwinski M, and Parkinson O (2013) Biotransformation of xenobiotics, in: *Casarett & Doull's Toxicology: The Basic Science of Poisons* (Klaassen CD ed), pp 185-367, McGraw-Hill, New York.

Penning TM and Drury JE (2007) Human aldo-keto reductases: Function, gene regulation, and single nucleotide polymorphisms. *Arch Biochem Biophys* **464:**241-250.

Ranhotra HS, Flannigan KL, Brave M, Mukherjee S, Lukin DJ, Hirota SA, and Mani S (2016) Xenobiotic receptor-mediated regulation of intestinal barrier function and innate immunity. *Nucl Receptor Res* **3:**pii: 101199.

Rizkallah MR, Gamal-Eldin S, and Saad R (2012) The PharmacoMicrobiomics Portal: A database for drug-microbiome interactions. *Curr Pharmacogenomics Person Med* **10:**195-203.

Sartor MA, Schnekenburger M, Marlowe JL, Reichard JF, Wang Y, Fan Y, Ma C, Karyala S, Halbleib D, Liu X, Medvedovic M, and Puga A (2009) Genomewide analysis of aryl hydrocarbon receptor binding targets reveals an extensive array

of gene clusters that control morphogenetic and developmental programs. *Environ Health Perspect* **117:**1139-1146.

Sayin SI, Wahlstrom A, Felin J, Jantti S, Marschall HU, Bamberg K, Angelin B, Hyotylainen T, Oresic M, and Backhed F (2013) Gut microbiota regulates bile acid metabolism by reducing the levels of tauro-beta-muricholic acid, a naturally occurring FXR antagonist. *Cell Metab* **17:**225-235.

Selwyn FP, Cheng SL, Klaassen CD, and Cui JY (2016) Regulation of hepatic drug-metabolizing enzymes in germ-free mice by conventionalization and probiotics. *Drug Metab Dispos* **44:**262-274.

Selwyn FP, Csanaky IL, Zhang Y, and Klaassen CD (2015a) Importance of large intestine in regulating bile acids and glucagon-like peptide-1 in germ-free mice. *Drug Metab Dispos* **43:**1544-1556.

Selwyn FP, Cui JY, and Klaassen CD (2015b) RNA-Seq Quantification of Hepatic Drug Processing Genes in Germ-Free Mice. *Drug Metab Dispos* **43:**1572-1580.

Stojancevic M, Bojic G, Salami HA, and Mikov M (2014) The Influence of Intestinal Tract and Probiotics on the Fate of Orally Administered Drugs. *Curr Issues Mol Biol* **16:**55-68.

Sugatani J (2013) Function, genetic polymorphism, and transcriptional regulation of human UDP-glucuronosyltransferase (UGT) 1A1. *Drug Metab Pharmacokinet* **28:**83-92.

Toda T, Saito N, Ikarashi N, Ito K, Yamamoto M, Ishige A, Watanabe K, and Sugiyama K (2009) Intestinal flora induces the expression of Cyp3a in the mouse liver. *Xenobiotica* **39:**323-334.

Tremaroli V and Backhed F (2012) Functional interactions between the gut microbiota and host metabolism. *Nature* **489:**242-249.

Venkatesh M, Mukherjee S, Wang H, Li H, Sun K, Benechet AP, Qiu Z, Maher L, Redinbo MR, Phillips RS, Fleet JC, Kortagere S, Mukherjee P, Fasano A, Le Ven J, Nicholson JK, Dumas ME, Khanna KM, and Mani S (2014) Symbiotic bacterial metabolites regulate gastrointestinal barrier function via the xenobiotic sensor PXR and Toll-like receptor 4. *Immunity* **41:**296-310.

Wahlstrom A, Sayin SI, Marschall HU, and Backhed F (2016) Intestinal Crosstalk between Bile Acids and Microbiota and Its Impact on Host Metabolism. *Cell Metab* **24:**41-50.

Wilkinson GR (1996) Cytochrome P4503A (CYP3A) metabolism: prediction of in vivo activity in humans. *J Pharmacokinet Biopharm* **24:**475-490.

Zaphiropoulos PG (2003) A map of the mouse Cyp3a locus. *DNA Seq* **14:**155-162.

Zhang Y, Cheng X, Aleksunes L, and Klaassen CD (2012) Transcription factor-mediated regulation of carboxylesterase enzymes in livers of mice. *Drug Metab Dispos* **40:**1191-1197.

Footnotes

This work was supported by the National Institute of General Medical Sciences [GM111381], National Institutes of Health National Institute of Environmental Health Sciences [ES025708, ES019487], as well as University of Washington Center for Ecogenetics and Environmental Health [P30 ES007033].

Figure legends

Fig. 1. Two-way hierarchical clustering of XPGs with differential expression between CV and GF. Various sections of the intestine (duodenum or duo, jejunum or jej, ileum or ile, as well as large intestine or LI) from C57BL/6J CV and GF male mice of ages 2-3 months were used for RNA-Seq quantification. The heatmap dendrogram describes XPG expression profiles between CV and GF mice in various intestine sections (FDR-BH<0.05 by Cuffdiff analysis, in at least one section of the intestine). Average FPKM values of three mice per tissue are presented by colored squares: red, relatively high expression; blue, relatively low expression.

Fig. 2. The intestinal expression of Cess and Ephxs in GF mice. Data are represented as mean FPKM ± S.E.M. of three individual animals. Differences between CV and GF mice that were significant by Cuffdiff (FDR-BH<0.05) were represented with asterisks. Ces, carboxylesterase; Ephx, epoxide hydrolase.

Fig. 3. The intestinal expression of Akrs and Cbrs in GF mice. Data are represented as mean FPKM ± S.E.M. of three individual animals. Differences between CV and GF mice that were significant by Cuffdiff (FDR-BH<0.05) were represented with asterisks. Akr, aldo-keto reductase; Cbr, carbonyl reductase.

Fig. 4. The intestinal expression of some P450s (Cyp1 to Cyp4 family) and Por in GF mice. Data are represented as mean FPKM ± S.E.M. of three individual animals. Differences between CV and GF mice that were significant by Cuffdiff (FDR-BH<0.05) were represented with asterisks. P450, cytochrome P450; Por, P450 (cytochrome) oxidoreductase.

Fig. 5. The intestinal expression of Adhs, Aldhs, Aox1, and Fmos in GF mice. Data are represented as mean FPKM ± S.E.M. of three individual animals. Differences between CV and GF mice that were significant by Cuffdiff (FDR-BH<0.05) were represented with asterisks. Adh, alcohol dehydrogenase; Aldh, aldehyde dehydrogenase; Aox, aldehyde oxidase; Fmo, flavin monooxygenase.

Fig. 6. The intestinal expression of Ugts, Sults, and Nat2 in GF mice. Data are represented as mean FPKM ± S.E.M. of three individual animals. Differences between CV and GF mice that were significant by Cuffdiff (FDR-BH<0.05) were represented with asterisks. Ugt, UDP-glucuronosyltransferase; Sult, sulfotransferase; Nat, *N*-acetyltransferase.

Fig. 7. The intestinal expression of Gsts in GF mice. Data are represented as mean FPKM ± S.E.M. of three individual animals. Differences between CV and GF mice that were significant by Cuffdiff (FDR-BH<0.05) were represented with asterisks. Gst, glutathione *S*-transferase.

Fig. 8. The intestinal expression of phase-II conjugation cosubstrate synthetic enzymes in GF mice. Data are represented as mean FPKM ± S.E.M. of three individual animals. Differences between CV and GF mice that were significant by Cuffdiff (FDR-BH<0.05) were represented with asterisks. Ugp2, UDP-glucose pyrophosphorylase 2; Ugdh, UDP-glucose 6-dehydrogenase; Papss, 3'-phosphoadenosine 5'-phosphosulfate synthase; Gclc, glutamate-cysteine ligase catalytic subunit; Gclm, glutamate-cysteine ligase modifier subunit; Mat, methionine adenosyltransferase.

Fig. 9. The intestinal expression of uptake and efflux xenobiotic transporters in GF mice. Data are represented as mean FPKM ± S.E.M. of three individual animals. Differences between CV and GF mice that were significant by Cuffdiff (FDR-BH<0.05) were represented with asterisks. Ntcp, Na^+-taurocholate cotransporting polypeptide; Abst, apical sodium-dependent bile acid transporter; Pept, peptide transporter; Oct, organic cation transporter; Octn, organic cation/carnitine transporter; Cnt, concentrative nucleoside transporter; Ent, equilibrative nucleoside transporter; Oatp, organic anion transporting polypeptide; Mrp, multidrug resistance-associated protein; Abc; ATP-binding cassette; Mate, multidrug and toxin extrusion transporter; Ost, organic solute transporter.

Fig. 10. The intestinal expression of xenobiotic-related transcription factors in GF mice. Data are represented as mean FPKM ± S.E.M. of three individual animals. Differences between CV and GF mice that were significant by Cuffdiff (FDR-BH<0.05) were represented with asterisks. AhR, aryl hydrocarbon receptor; CAR, constitutive androstane receptor; FXR, farnesoid X receptor; HNF, hepatocyte nuclear factor; PPAR, peroxisome proliferator-activated receptor; PXR, pregnane X receptor; RXR, retinoid X receptor; Nrf2, nuclear factor erythroid 2-related factor 2.

DMD Fast Forward. Published on September 22, 2017 as DOI: 10.1124/dmd.117.077313
This article has not been copyedited and formatted. The final version may differ from this version.

Table 1. List of 116 XPGs that have differential expression (DE) between CV and GF mice in at least one section of the intestine (FDR-BH<0.05, Cuffdiff).

DE XPGs #		Duodenum (Duo)	Jejunum (Jej)	Ileum (Ile)	Large intestine (LI)
69 phase-I enzymes	8 Cess	Ces1d, 2a,	Ces1e, 1f, 2a, 2b	Ces2a, 2g	Ces1e, 1g, 2a, 2c, 2g
	3 Ephxs	Ephx1	Ephx1, 2	Ephx2	Ephx2, 4
	7 Akrs	Akr1c19	Akr1b7, 1c12, 1c13, 1c14, 1c19	Akr1c12, 1c13, 1c14, 1c19	Akr1b8, 1c12, 1c13, 1c14, 1c18, 1c19
	2 Cbrs		Cbr1		Cbr3
	30 P450s +Por	Cyp1a1, 2b10, 2c55, 2c66, 2d10, 3a11, 3a25, 3a44, 3a59, 4b1	Cyp1a1, 1b1, 2c38, 2c44, 2c55, 2c66, 2c67, 2c68, 2d26, 2e1, 2w1, 3a13, 4a10, 4b1, 4f13, 4f14, 4v3, Por	Cyp1a1, 2b10, 2c29, 2c55, 2c65, 2c66, 2j9, 3a11, 3a25, 3a59, 4b1	Cyp2d13, 2c55, 2c65, 2c66, 2d9, 2d10, 2d12, 2d26, 2d34, 2w1, 3a13, 4b1, 4f14, 4v3
	6 Adhs	Adh1l2	Adh1, 4, 6a, 7, fe1,	Adh1, 4, 6a	Adh5
	9 Aldhs	Aldh4a1, 18a1	Aldh1a1, 1l1, 3a2, 3b1, 4a1		Aldh1a1, 1a7, 1b1, 1l2
	3 Fmos	Fmo2	Fmo4, 5		Fmo5
27 phase-II enzymes	5 Ugts	Ugt2b38	Ugt2a3		Ugt1a1, 2b5, 2b36
	5 Sults	Sult1c2	Sult1b1, 1c2, 1d1, 2b1, 4a1	Sult2b1	Sult1c2
	12 Gsts	Gsta1, m1, m3, m4	Gsta1, a4, k1, m6, m7, o1, p1, t1	Gstk1, m1, m3, m4, m6, t1	Gsta3, o1
	1 Nat		Nat2		
	4 enzymes for cofactors		Ugdh, Papss2, Gclm	Gclc	Ugdh, Gclc
17 transporters	11 Uptake	Cnt2	Asbt, Pept1, Oct1, Oct3, Octn2, Cnt1, Cnt2, Ent4, Oatp2a1, Oatp3a1	Asbt, Cnt1, Cnt2	Asbt, Pept1, Octn1, Cnt2, Oatp2a1
	6 Efflux	Mate1	Mrp2, 7, Mate1	Mrp6	Mrp6, Ostα, Ostβ
3 TFs			FXR, PPARα, PXR,		FXR

Table 2. List of 54 XPGs that are not expressed (NE) in the intestine of CV or GF mice (FPKM<1 in all sections of the intestine).

NE XPGs #		XPGs
21 phase-I enzymes	4 Cess	Ces1a, 2f, 4a, 5a
	1 Ephx	Ephx3
	1 Akr	Akr1c21
	2 Nqos	Nqo1, Nqo2
	11 P450s	Cyp2b9, 2b19, 2b23, 2c39, 2g1, 2j5, 2j8, 2j11, 2t4, 4f39, 4x1
	1 Aox	Aox3l1
	1 Fmo	Fmo3
18 phase-II enzymes	4 Ugts	Ugt1a2, 1a10, 2a1, 2a2
	10 Sults	Sult1c1, 1e1, 2a1, 2a2, 2a3, 2a4, 2a5, 2a7, 3a1, 6b1
	2 Gsts	Gsto2, t4
	2 Nats	Nat1, 3
15 transporters	13 Uptake	Ntcp, Oct2, Oat1, Oat3, Urat1, Oatp1a5, 1a6, 1c1, 4c1, 5a1, 6b1, 6c1, 6d1
	2 Efflux	Mrp9, Mate2

DMD Fast Forward. Published on September 22, 2017 as DOI: 10.1124/dmd.117.077313
This article has not been copyedited and formatted. The final version may differ from this version.

Table 3. List of 133 XPGs with no differential expression (NDE) in the intestine between CV and GF mice (FDR-BH≥0.05, Cuffdiff).

NDE XPGs #		XPGs
68 phase-I enzymes	6 Cess	Ces1b, 1c, 2e, 2h, 3a, 3b
	3 Pons	Pon1, 2, 3
	8 Akrs	Akr1a4, 1b3, 1b10, 1c6, 1c20, 1d1, 1e1, 7a5
	2 Cbrs	Cbr2, 4
	35 P450s	Cyp1a2, 2a4, 2a5, 2a12, 2a22, 2b13, 2c37, 2c40, 2c50, 2c54, 2c69, 2c70, 2d11, 2d22, 2d40, 2f2, 2j6, 2j13, 2r1, 2s1, 2u1, 3a16, 3a41a, 3a57, 4a12a, 4a12b, 4a14, 4a31, 4a32, 4f15, 4f16, 4f17, 4f18, 4f37, 4f40
	11 Aldhs	Aldh1a2, 1a3, 2, 3a1, 3b2, 5a1, 6a1, 7a1, 8a1, 9a1, 16a1
	2 Aoxs	Aox1, 3
	1 Fmo	Fmo1
33 phase-II enzymes	9 Ugts	Ugt1a5, 1a6a, 1a6b, 1a7c, 1a9, 2b1, 2b34, 2b35, 2b37
	2 Sults	Sult1a1, 5a1
	11 Gsts	Gsta2, cd, m2, m5, p2, t2, t3, z1, Mgst1, 2, 3
	3 methyl transferase	Comt, As3mt, Tpmt
	3 Amino acid-conjugation enzymes	Bal, Bat, Glyat
	5 enzymes for cosubstrates	Ugp2, Papss1, Mat1a, 2a, 2b
24 transporters	12 Uptake	Pept2, Octn3, Oat2, Cnt3, Ent1, 2, 3, Oatp1a1, 1a4, 1b2, 2b1, 4a1
	12 Efflux	Abca1, Mdr1a, 1b, Mdr2, Bsep, Mrp1, 3, 4, 5, Bcrp, Abcg5, g8
8 TFs		AhR, CAR, HNF1α, 4α, RXRα, β, γ, Nrf2

DMD Fast Forward. Published on September 22, 2017 as DOI: 10.1124/dmd.117.077313
This article has not been copyedited and formatted. The final version may differ from this version.

Table 4. List of XPGs that have over 5-fold differential expression in GF vs CV mice in at least one section of the intestine.

DE XPGs #	Increase	Decrease
8 phase-I enzymes	Akr1c18 (LI) Cyp2d26 (LI) Aldh4a1 (Jej)	Cyp1a1 (Duo, Jej, Ile) Cyp2c29 (Ile) Cyp2c55 (Ile) Cyp2c66 (Ile) Cyp3a11 (Ile)
1 phase-II enzyme	Ugt1a1 (LI)	
3 transporters	Asbt (LI) Octn1 (LI) Ostα (LI)	Asbt (Jej)

DMD Fast Forward. Published on September 22, 2017 as DOI: 10.1124/dmd.117.077313
This article has not been copyedited and formatted. The final version may differ from this version.

Figure 1

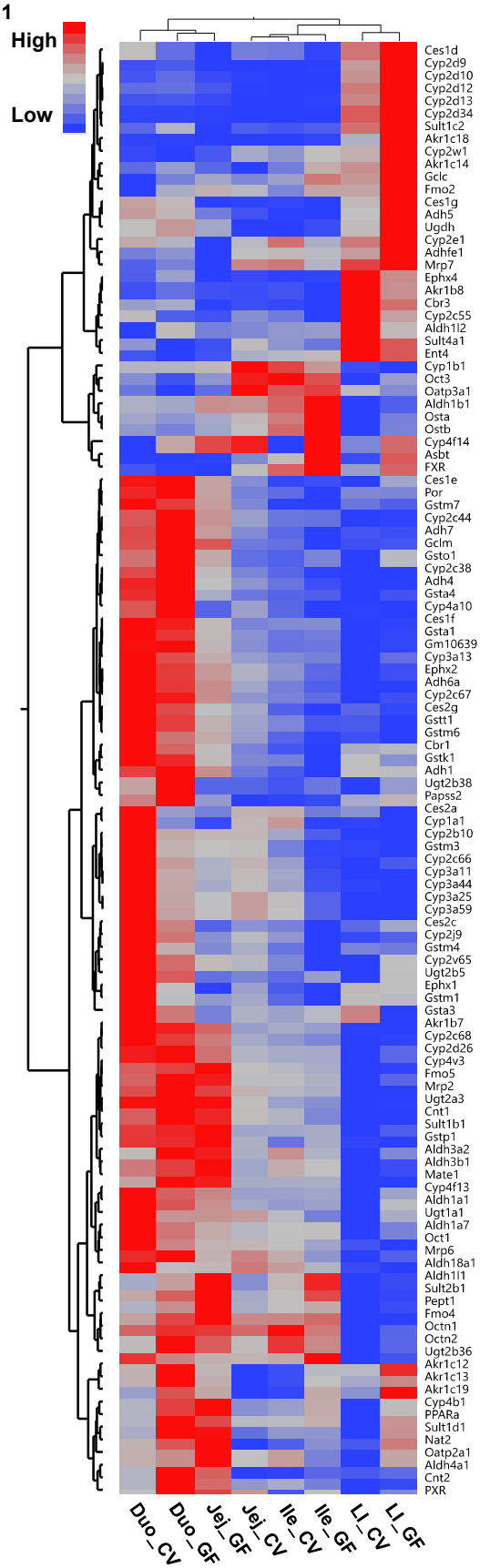

DMD Fast Forward. Published on September 22, 2017 as DOI: 10.1124/dmd.117.077313
This article has not been copyedited and formatted. The final version may differ from this version.

Figure 2

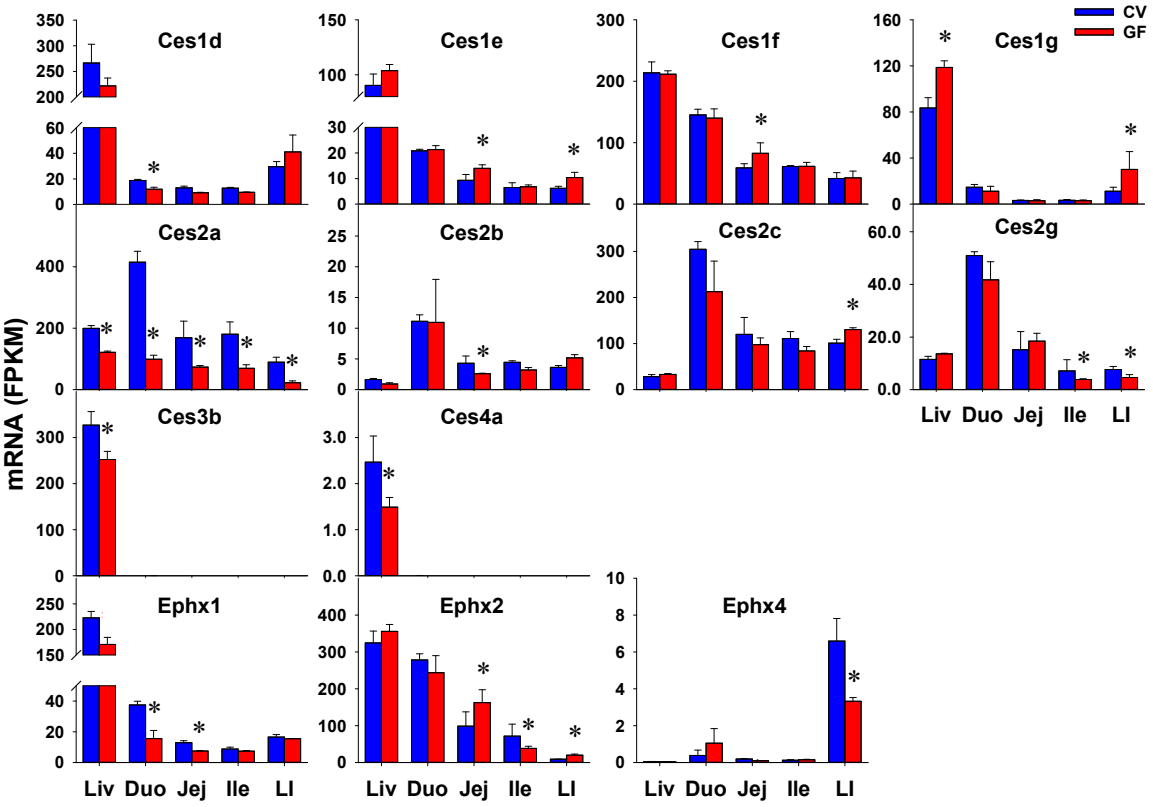

Figure 3

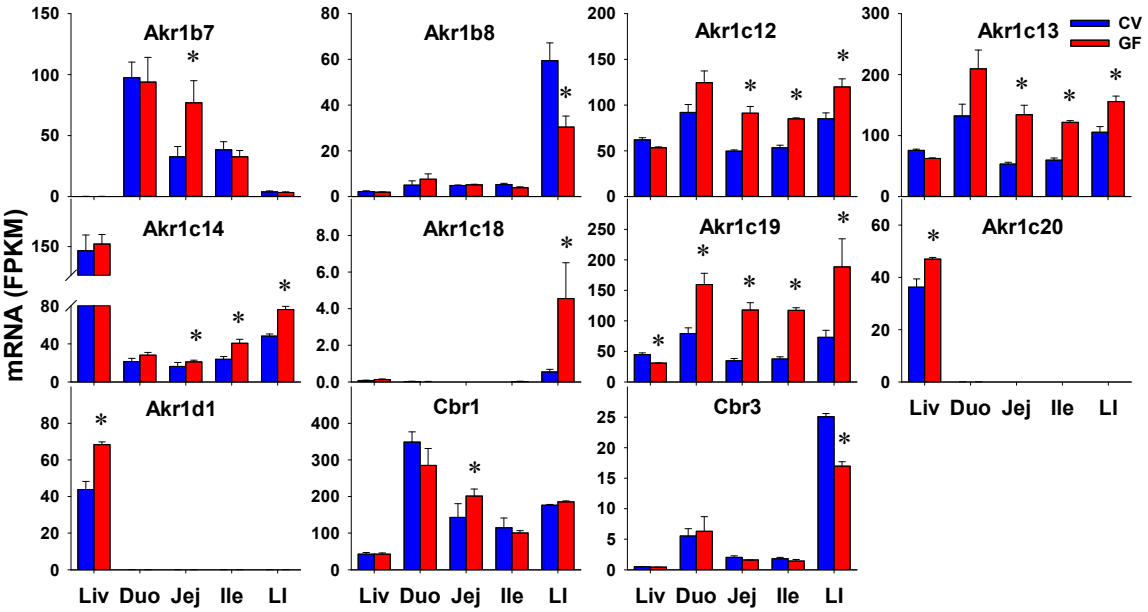

DMD Fast Forward. Published on September 22, 2017 as DOI: 10.1124/dmd.117.077313
This article has not been copyedited and formatted. The final version may differ from this version.

Figure 4
(A)

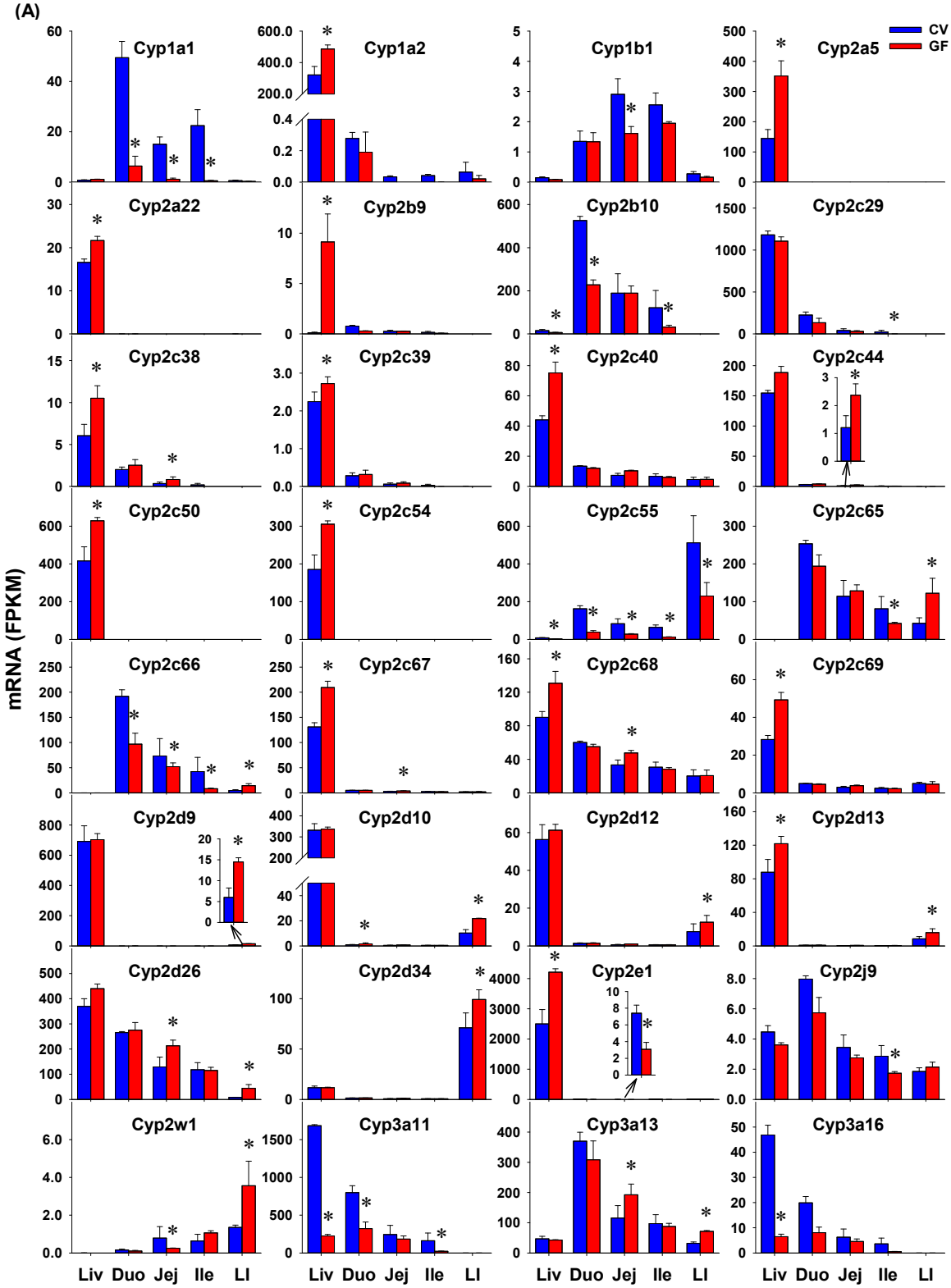

DMD Fast Forward. Published on September 22, 2017 as DOI: 10.1124/dmd.117.077313
This article has not been copyedited and formatted. The final version may differ from this version.

Figure 4
(B)

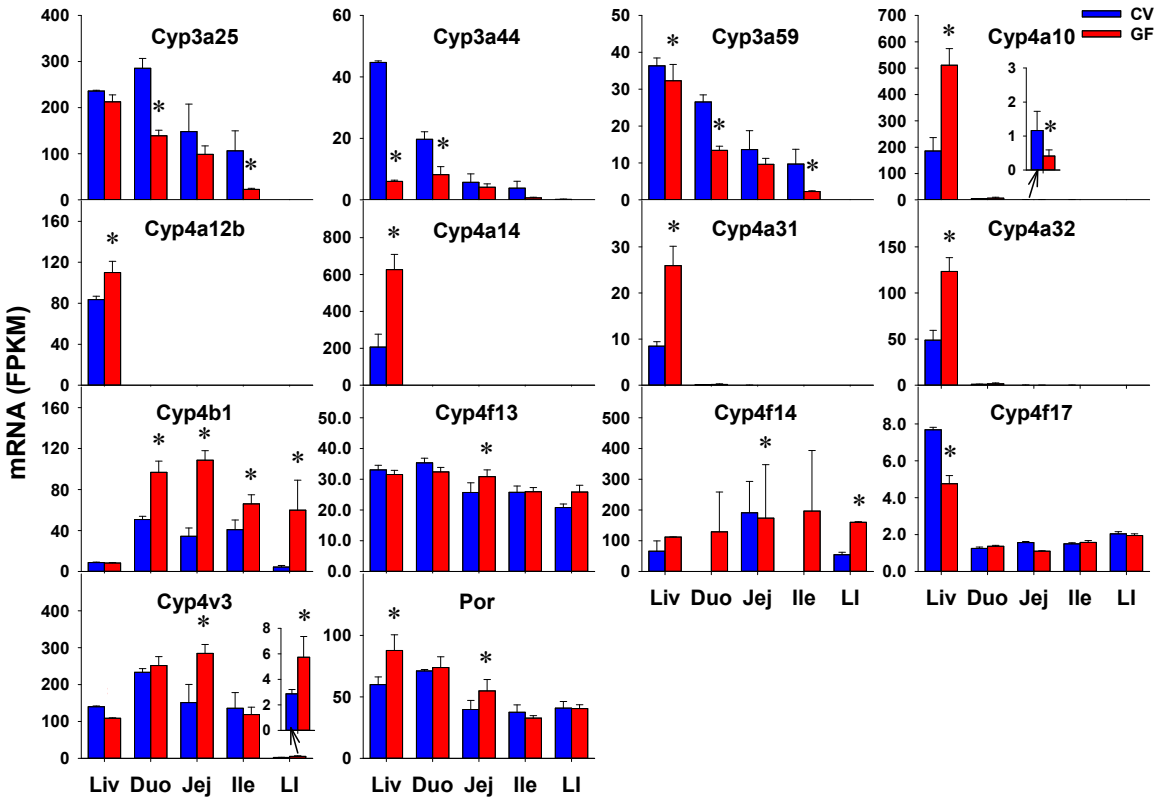

DMD Fast Forward. Published on September 22, 2017 as DOI: 10.1124/dmd.117.077313
This article has not been copyedited and formatted. The final version may differ from this version.

Figure 5

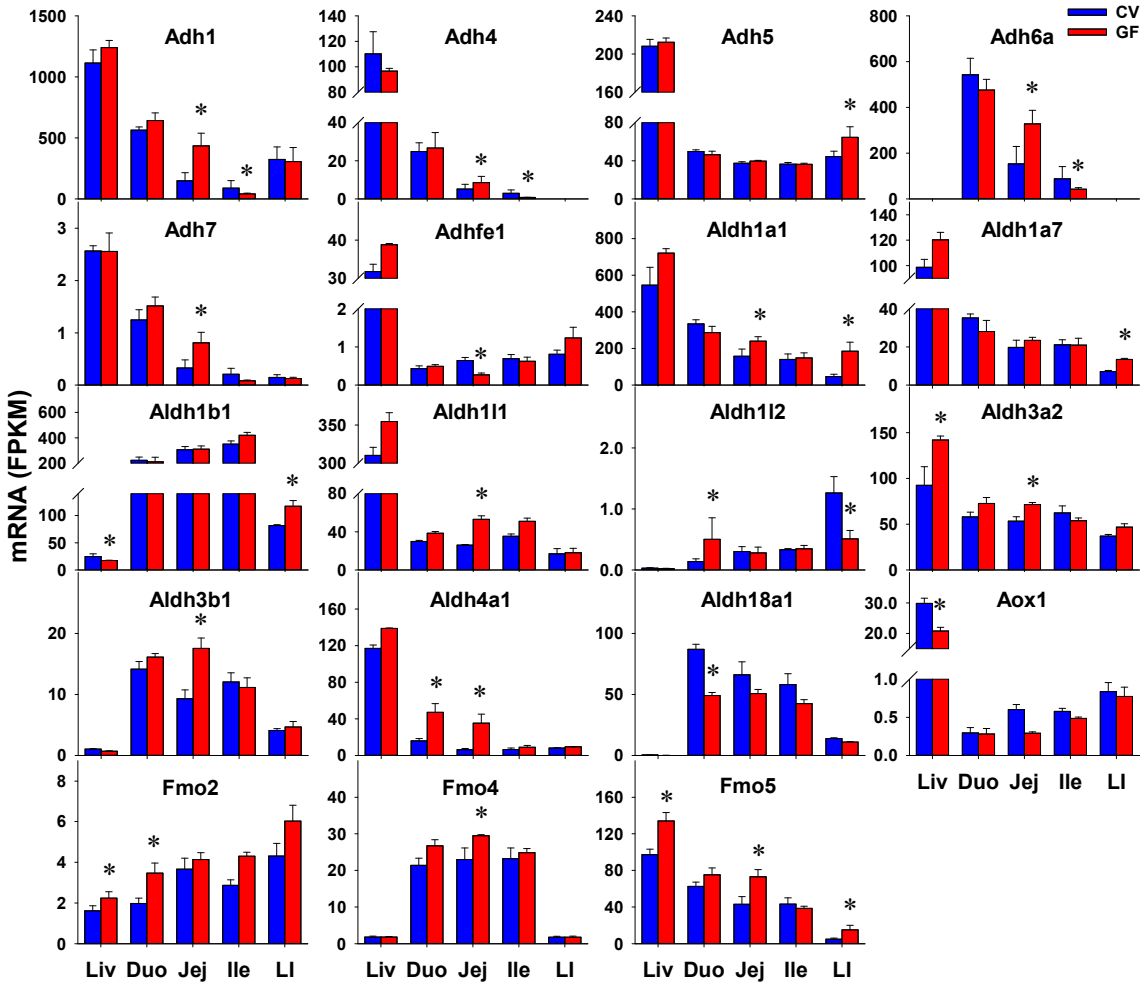

DMD Fast Forward. Published on September 22, 2017 as DOI: 10.1124/dmd.117.077313
This article has not been copyedited and formatted. The final version may differ from this version.

Figure 6

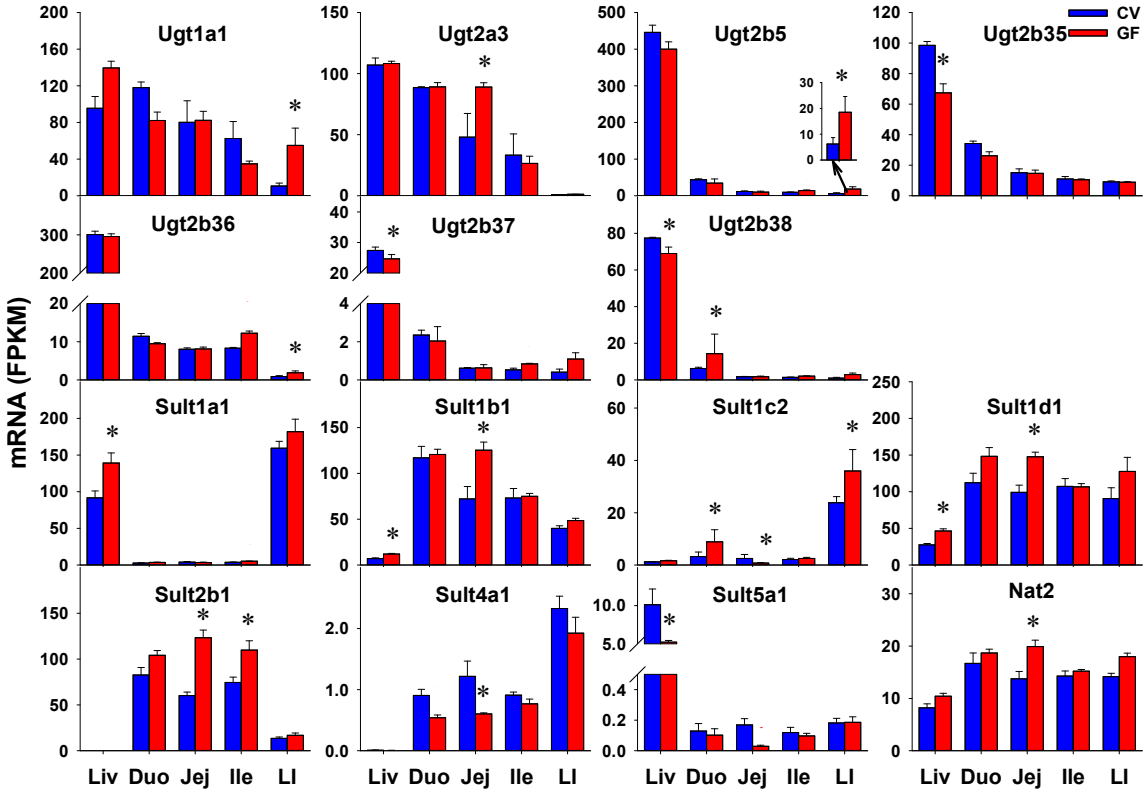

DMD Fast Forward. Published on September 22, 2017 as DOI: 10.1124/dmd.117.077313
This article has not been copyedited and formatted. The final version may differ from this version.

Figure 7

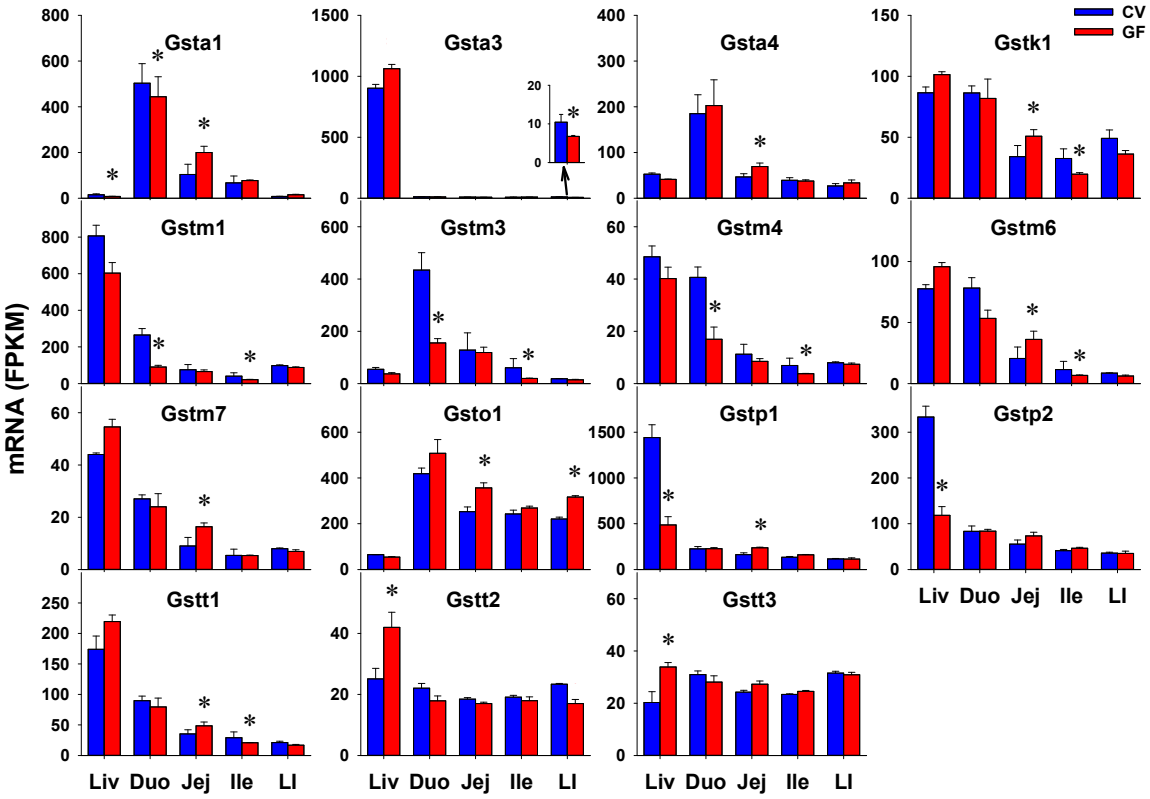

DMD Fast Forward. Published on September 22, 2017 as DOI: 10.1124/dmd.117.077313
This article has not been copyedited and formatted. The final version may differ from this version.

Figure 8

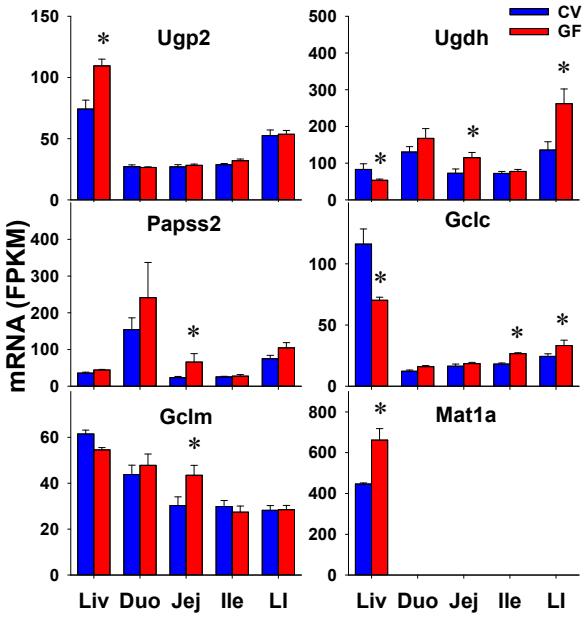

DMD Fast Forward. Published on September 22, 2017 as DOI: 10.1124/dmd.117.077313
This article has not been copyedited and formatted. The final version may differ from this version.

Figure 9

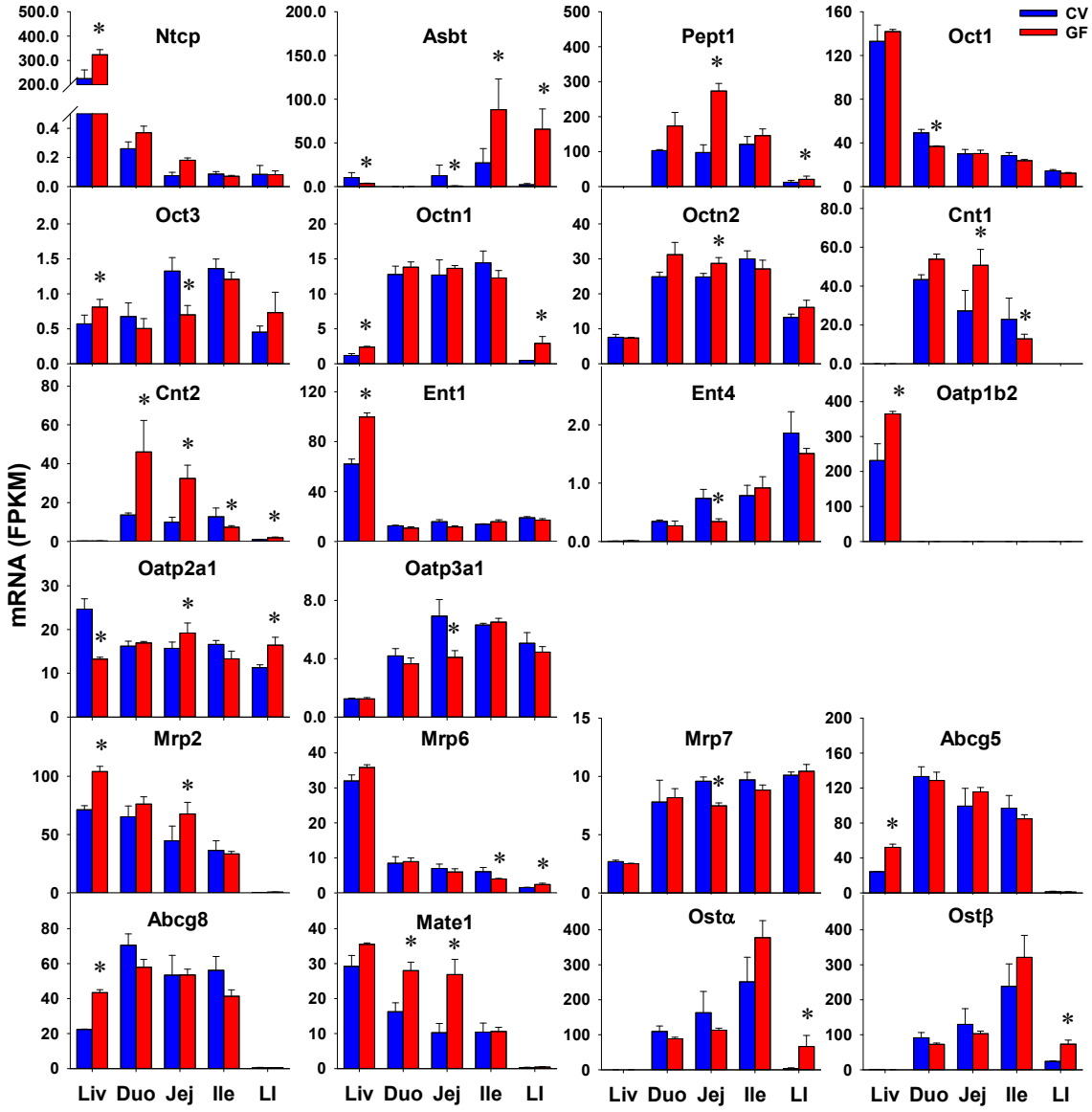

DMD Fast Forward. Published on September 22, 2017 as DOI: 10.1124/dmd.117.077313
This article has not been copyedited and formatted. The final version may differ from this version.

Figure 10